

		Volume 72, Number 9 May 1, 2008		
		<h1 style="margin: 0;">Geochimica et Cosmochimica Acta</h1> <p style="margin: 0;">JOURNAL OF THE GEOCHEMICAL SOCIETY AND THE METEORITICAL SOCIETY</p>		
Executive Editor: FRANK A. PODOSEK		Editorial Manager: LINDA TOWER Editorial Assistant: KATHI KLATZ KATHI SUZUKI		
		Webmaster: ROBERT H. NICHOLS, JR. Production Manager: CHRIS ALGER		
ASSOCIATE EDITORS: ROBERT C. ALLEN JEFFREY C. ALP YOSHIO ANDO CAROL ANTONIO MERTON BIRN MATTIERS LIONEL G. BREWER THOMAS S. BRIDGES JAY A. BRONSON ALAN D. BRONSON DAVID J. BRONSON ROBERT C. BRIDGES WILLIAM H. CROFT THOMAS CHAPMAN ANNE CHAPMAN DAVID R. COLE	LAURA J. COOPER JOHN CHERRY CHRISTOPHER DAGGAMBY ZHENGLIANG DING JAMES FARVER FREDERICK A. FERT FRANCIS R. HALL T. MARK HARRISON H. ROBERT HARTY GEORGE R. HEZEL GEORGE F. HERTZOG JOSE HERRERA JUN-ICHIRO HIRAI KIMMO IJANEN CLARK JARVIS NORIKO KITA	CHRISTIAN KORBEL RICHARD KORTY SUZUKI M. KIKUCHI S. KIKUCHI ALFONSO M. KILIAN JAMES KILIAN TOSHIOKI KISHIMOTO GEORGE A. LAGAN TOSHIOKI KISHIMOTO MICHAEL L. MCGEEHRY JIN-ICHI MATSUDA JAMES McMONAGHAN ANTON MERTON MARTIN A. MURPHY JACK J. MURPHY	DAVID W. METZLER ALFONSO MICHETTI HIDEO MIYATA HIROSHI NAGAIWA MARTIN NYQUIST PIERRE A. OUDOT ERIC H. OHLBERG SANDRO PIZZAGALLO MILOJKA RANJBAR W. ULRICH REINOLD ERIC M. RIEDEL J. KELLY RUSSELL SARA S. RUSSELL JAMES R. RUTHERFORD F. J. RYAN JOCKIE SCOTT	JEFFREY SHEPHERD TREVOR J. SIMP J. S. SNOOK DAVID L. SODERBERG GABRIEL SODERBERG DAVID A. SWANSON MICHAEL J. TOPPER PETER TRUDEL DAVID J. VAGNER RICHARD J. WALKER LARRY A. WATSON JAMES WATSON KAREN WELLS ROY A. WOODHEAD CHEN ZHANG
Volume 72, Number 9		May 1, 2008		
Articles				
I. C. BOURO, G. SPONTO: Isotopic fractionation of noble gases by diffusion in liquid water: Molecular dynamics simulations and hydrologic applications		2237		
S. T. GOLDSMITH, A. E. CAREY, W. B. LYONS, D. M. HECK: Geochemical fluxes and weathering of volcanic terrains on high standing islands: Taranaki and Manawatu-Wanganui regions of New Zealand		2248		
P. LAM, J. P. COWEN, B. N. POPP, R. D. JONES: Microbial ammonia oxidation and enhanced nitrogen cycling in the Endeavour hydrothermal plume		2268		
M. A. DONAHUE, J. P. WORSNE, C. MEILL, T. W. LYONS: Modeling sulfur isotope fractionation and differential diffusion during sulfate reduction in sediments of the Cariaco Basin		2287		
S. DATTA GUPTA, M. A. ARTHUR, C. R. FISHER: Modification of sediment geochemistry by the hydrocarbon seep tubeworm <i>Lamellibrachia kellyi</i> : A combined empirical and modeling approach		2298		
T. ULKUCI, J. MATHIEN: An experimental study of the solubility of molybdenum in H ₂ O and KCl-H ₂ O solutions from 500 °C to 800 °C, and 150 to 300 MPa		2316		
X. XIE, M. KANZAKI: Structure of hydrous aluminosilicate glasses along the diopside-anorthite join. A comprehensive one- and two-dimensional ¹ H and ²⁷ Al NMR study		2331		
Y. LIU, S. GAO, P. B. KELEMEK, W. XU: Recycled crust controls contrasting source compositions of Mesozoic and Cenozoic basalts in the North China Craton		2349		
S. MEFFRE, R. R. LARUE, R. SCOTT, J. WOODHEAD, Z. CHANG, S. E. GILBERT, L. V. DASYUBREVSKY, V. MASLENNIKOV, J. M. HEROT: Age and pyrite Pb-isotopic composition of the giant Sakhalin Log sediment-hosted gold deposit, Russia		2377		
A. V. BOBKOV, H. KOHTANI, M. AKAGI, Y. A. LITVIN: Phase relations on the diopside-jadeite-hedenbergite join up to 24 GPa and stability of Na-bearing majoritic garnet		2392		
<i>Continued on outside back cover</i>				

This article appeared in a journal published by Elsevier. The attached copy is furnished to the author for internal non-commercial research and education use, including for instruction at the authors institution and sharing with colleagues.

Other uses, including reproduction and distribution, or selling or licensing copies, or posting to personal, institutional or third party websites are prohibited.

In most cases authors are permitted to post their version of the article (e.g. in Word or Tex form) to their personal website or institutional repository. Authors requiring further information regarding Elsevier's archiving and manuscript policies are encouraged to visit:

<http://www.elsevier.com/copyright>



Modeling sulfur isotope fractionation and differential diffusion during sulfate reduction in sediments of the Cariaco Basin

Michael A. Donahue^a, Josef P. Werne^{a,b,*}, Christof Meile^c, Timothy W. Lyons^d

^a Large Lakes Observatory, University of Minnesota Duluth, 10 University Dr., 109 RLB, Duluth, MN 55812, USA

^b Department of Chemistry & Biochemistry, University of Minnesota Duluth, Duluth, MN 55812, USA

^c Department of Marine Science, University of Georgia, Athens, GA 30602, USA

^d Department of Earth Sciences, University of California, Riverside, CA 92521, USA

Received 14 March 2007; accepted in revised form 20 February 2008; available online 12 March 2008

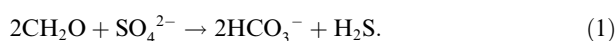
Abstract

Sulfur isotope composition ($\delta^{34}\text{S}$) profiles in sediment pore waters often show an offset between sulfate and sulfide ($\Delta\delta^{34}\text{S}_{\text{SO}_4\text{-H}_2\text{S}}$) much greater in magnitude than S isotope fractionations observed in pure cultures. A number of workers have invoked an additional reaction, microbial disproportionation of sulfur intermediates, to explain the offset between experimental and natural systems. Here, we present an alternative explanation based on modeling of pore water sulfate and sulfide concentrations and stable isotope data from the Cariaco Basin (ODP Leg 165, Site 1002B). The use of unique diffusion coefficients for $^{32}\text{SO}_4^{2-}$ and $^{34}\text{SO}_4^{2-}$, based on their unequal molecular masses, resulted in an increase in the computed fractionation by almost 10‰, when compared to the common assumption of equal diffusion coefficients for the two species. These small differences in diffusion coefficients yield calculated isotopic offsets between coeval sediment pore water sulfate and sulfide without disproportionation (up to 53.4‰) that exceed the largest fractionations observed in experimental cultures. Furthermore, the diffusion of sulfide within sediment pore waters leads to $\Delta\delta^{34}\text{S}_{\text{SO}_4\text{-H}_2\text{S}}$ values that are even greater than those predicted by our model for sulfate reduction with unique diffusion coefficients. These diffusive effects on the sulfur isotope composition of pore water sulfate and sulfide can impact our interpretations of geologic records of sulfate and sulfide minerals, and should be considered in future studies.

© 2008 Published by Elsevier Ltd.

1. INTRODUCTION

Microbial sulfate reduction (SR) is globally the most important anaerobic pathway for organic matter decomposition in marine sediments (Canfield et al., 1993) and couples the carbon and sulfur cycles according to the generalized equation (Berner, 1984):



Sulfate-reducing bacteria preferentially utilize sulfate that contains ^{32}S during metabolism, resulting in the production of dissolved sulfide that is depleted in ^{34}S relative to sulfate. This ^{34}S -depleted sulfide formed during microbial sulfate reduction can react with iron to form iron sulfides and ultimately pyrite (FeS_2), which is the primary sink for reduced sulfur from the oceans (Berner, 1982). Since the sulfur isotope fractionation associated with pyrite formation is less than 1‰ (Price and Shieh, 1979), the pyrite records the isotopic composition ($\delta^{34}\text{S}$) of the sulfide from which it was formed. Similarly, gypsum ($\text{CaSO}_4 \cdot 2\text{H}_2\text{O}$), barite (BaSO_4), and carbonate-associated sulfate preserved in the geologic record track the $\delta^{34}\text{S}$ of seawater sulfate from which they were created, with a small offset (Thode

* Corresponding author. Fax: +1 218 728 6979.
E-mail address: jwerne@d.umn.edu (J.P. Werne).

and Monster, 1965; Holser and Kaplan, 1966; Paytan et al., 1998; Kah et al., 2004). Thus, the sulfur isotope offset between seawater sulfate and sulfide ($\Delta\delta^{34}\text{S}_{\text{SO}_4\text{-H}_2\text{S}}$) is documented over geologic time via preservation in sedimentary sulfur minerals. Numerous workers have used this sulfur isotope offset between reduced and oxidized forms to infer both atmospheric and oceanic redox state and chemical evolution since the Precambrian (e.g., Garrels and Lerman, 1984; Berner and Petsch, 1998). Similarly, some have used the $\Delta\delta^{34}\text{S}_{\text{SO}_4\text{-H}_2\text{S}}$ in the global ocean to deduce oceanic sulfate concentrations following the assumption that a small offset and thus low fractionation during bacterial sulfate reduction reflects low sulfate concentrations (Habicht et al., 2002; Fike et al., 2006). An improved understanding of the mechanisms that generate the isotopic offset between pore water sulfate and sulfide in sedimentary marine systems therefore has the potential to provide information about the chemical evolution of the Earth.

The sulfur isotope fractionation imparted during microbial sulfate reduction (ϵ_{SR}) has been studied extensively in culture and generally lies between 2‰ and 47‰ (Harrison and Thode, 1958; Kaplan and Rittenberg, 1964; Kemp and Thode, 1968; Chambers et al., 1975; Habicht and Canfield, 1997; Detmers et al., 2001). ϵ_{SR} is controlled by a number of factors, including sulfate reduction rate, sulfate concentration, organic matter oxidation pathway, and the species of sulfate reducer (Brüchert, 2004, and references therein). The rate of sulfate reduction per cell is thought to be the principal factor governing the extent of isotope fractionation by sulfate-reducing bacteria (Canfield, 2001a). In pure culture studies an inverse relationship is generally encountered with the highest fractionations found at the lowest cell specific rates of sulfate reduction (Harrison and Thode, 1958; Kaplan and Rittenberg, 1964), although this is not a simple relationship when extrapolated to complex natural systems with greater microbial diversity (Detmers et al., 2001).

Briefly, SR is a multi-step reaction, and the maximum fractionation will be expressed when all of the intermediates involved in this reaction are in exchange equilibrium (Kaplan and Rittenberg, 1964; Rees, 1973; Canfield, 2001a; Brunner and Bernasconi, 2005). Maintaining exchange equilibrium among all of the intermediate species in SR is best accomplished when the specific rate of sulfate reduction is kept low, leading to the overall observed trend of high S isotope fractionations associated with low cell specific rates. However, slow rates of SR are not required to achieve large S isotope fractionations, as long as the backflux is large (Brunner and Bernasconi, 2005). Indeed, recent work suggests that the maximum theoretical sulfur isotope fractionation is on the order of 70‰ (Brunner and Bernasconi, 2005; Johnston et al., 2007). Furthermore, other experiments have shown that sulfate reducing bacteria that oxidize organic matter to acetate have fractionations less than 18‰, while reducers that are capable of oxidizing organic substrate to CO_2 consistently fractionate higher than 18‰ (Detmers et al., 2001). Consequently, a shift in the dominant species of sulfate reducer can have a large impact on the observed ϵ_{SR} . In addition, reduced isotope fractionation at sulfate concentrations < 1 mM (Harrison and

Thode, 1958; Canfield, 2001b) might be caused by a change in metabolic pathway and reduced growth yield (Habicht et al., 2005).

$\delta^{34}\text{S}$ profiles in the sediment pore waters often show much larger offsets between sulfate and sulfide than are expected based on the fractionation observed in pure cultures (as high as 60–70‰ compared to 2–47‰ in pure cultures; Canfield and Thamdrup, 1994; Brüchert, 2004). The recent discovery of bacteria that can disproportionate sulfur intermediates (i.e., elemental sulfur and thiosulfate) into sulfate and sulfide has provided a possible mechanism for generating such a large offset (Jørgensen, 1990a,b; Fossing and Jørgensen, 1990; Canfield and Thamdrup, 1994; Habicht et al., 1998). A scheme consisting of fractionation during bacterial sulfate reduction, followed by the (1) oxidation of sulfide to an intermediate state, (2) disproportionation of the sulfur intermediate compound, and (3) subsequent repeated cycles of partial oxidation and disproportionation has been proposed as a mechanism for generating the high $\Delta\delta^{34}\text{S}_{\text{SO}_4\text{-H}_2\text{S}}$ values observed in sedimentary environments (Canfield and Thamdrup, 1994). This additional pathway of fractionation may also explain sulfur isotope patterns seen in ancient sediments (Canfield and Teske, 1996; Johnston et al., 2005; Philippot et al., 2007).

$\delta^{34}\text{S}$ profiles of pore water sulfate and sulfide often show parallel increasing values with depth. This trend resembles one that would be expected from diagenesis under closed system conditions and led to the initial conclusion that sediments were governed by Rayleigh distillation isotope systematics (Nakai and Jensen, 1964). Since then, the roles of advective and diffusive transport in governing isotopic pore water signatures have been clearly demonstrated (e.g., Jørgensen, 1979; Bottrell and Raiswell, 2000) and applied to diverse sedimentary systems (Fossing et al., 2000; Böttcher et al., 2004; Jørgensen et al., 2004).

Here we present the results from a diagenetic modeling study of sediments collected in the Cariaco Basin, an anoxic setting with no sulfate limitation in either the water column or the upper 6 m of sediment. This environment is characterized by sulfur cycling with ample organic matter and sulfate but limited availability of oxidants in the sediments (Werne et al., 2003; Lyons et al., 2003). Such a system reduces the number of controlling variables and thus places the emphasis on transport processes, which are limited to molecular diffusion and advection through sedimentation. The microbial sulfate reduction rate, the S isotope fractionation associated with sulfate reduction, and the isotopic composition of H_2S in the Cariaco Basin were calculated, taking into account potential differences in the diffusion coefficients for $^{32}\text{SO}_4^{2-}$ versus $^{34}\text{SO}_4^{2-}$. Our findings suggest the potential for a large sulfur isotope fractionation associated with microbial sulfate reduction under strict anoxic conditions and specifically offer an explanation for an observed isotopic offset between sulfate and sulfide that is considerably larger than the modeled fractionation. Furthermore, our results highlight the significant impact of small but systematic differences in diffusion coefficients on the accuracy of diagenetic models of pore water isotopic species. These results suggest that the interpretation of large offsets between the $\delta^{34}\text{S}$ values of sulfate and sulfide miner-

als in the geologic record as indicative of the oxidative side of the sulfur cycle may need to be reassessed.

2. METHODS

2.1. Site description and sampling

The Cariaco Basin is a pull-apart basin located on the continental shelf north of Venezuela (Fig. 1). It consists of two sub-basins, each with a maximum depth of about 1400 m, separated by a saddle at 900 m. The Cariaco Basin is currently anoxic below approximately 300 m water depth and has been anoxic for the last 14,000 calendar years (Peterson et al., 1991). The presence of laminae and thus the lack of benthic fauna during the last 14,000 calendar years (Peterson et al., 1991; Hughen et al., 1996; Werne et al., 2000) indicate that bioturbation and bioirrigation are absent. The sedimentation rate has been approximately 30 cm/1000 years from 11,000 calendar years to the present (Hughen et al., 1996; see Werne et al., 2003; and Lyons et al., 2003, for further details). The data used in this study were generated from samples collected from ODP Site 165 (Core 1002B) at about 900 m water depth (Shipboard Scientific Party, 1997; see Werne et al., 2003 for the analytical methods).

2.2. Model development

Considering diffusion, advection, and reaction, the diagenetic mass conservation equation can be expressed as (Bernier, 1964):

$$\frac{\partial \phi C}{\partial t} = \frac{\partial}{\partial z} \left(D_{\text{sed}} \phi \frac{\partial C}{\partial z} \right) - \frac{\partial}{\partial z} (\omega \phi C) + \phi \sum R_i, \quad (2)$$

where C is the concentration of a dissolved species, t is time, D_{sed} is the whole sediment diffusion coefficient of a given species, z is depth, ϕ is the sediment porosity, ω is the sedimentation rate, and $\sum R_i$ is the sum of the individual reaction rates for the production and consumption of a given constituent. Note that Eq. (2) assumes the absence of additional transport processes such as bioturbation or advective flow, which is reasonable given the persistently anoxic conditions. Because deposition in the Cariaco Basin varied little over the last 10 ka years (Hughen et al., 1996; Werne et al., 2000), it is assumed that the system has had sufficient time to reach an approximate steady-state. For sulfate and sulfide concentration profiles at steady state ($\partial C/\partial t = 0$), the net rate of production or consumption is equal to the transport terms, expressed as:

$$\phi \sum R_i = - \frac{\partial}{\partial z} \left(D_{\text{sed}} \phi \frac{\partial C}{\partial z} \right) + \frac{\partial}{\partial z} (\omega \phi C). \quad (3)$$

In contrast to Jørgensen (1979), who measured microbial sulfate reduction rates and used literature values for the associated fractionation to generate theoretical concentration profiles, we use observed concentration and isotopic profiles of sulfate and sulfide to estimate net bacterial sulfate reduction rate ($\sum R_i$) and sulfur isotope fractionation for the Cariaco Basin sediment. In further contrast to previous studies (cf. Jørgensen, 1979; Fossing et al., 2000; Jørgensen et al., 2004), we also consider the isotope mass effect on diffusion coefficients of $^{32}\text{SO}_4^{2-}$ and $^{34}\text{SO}_4^{2-}$.

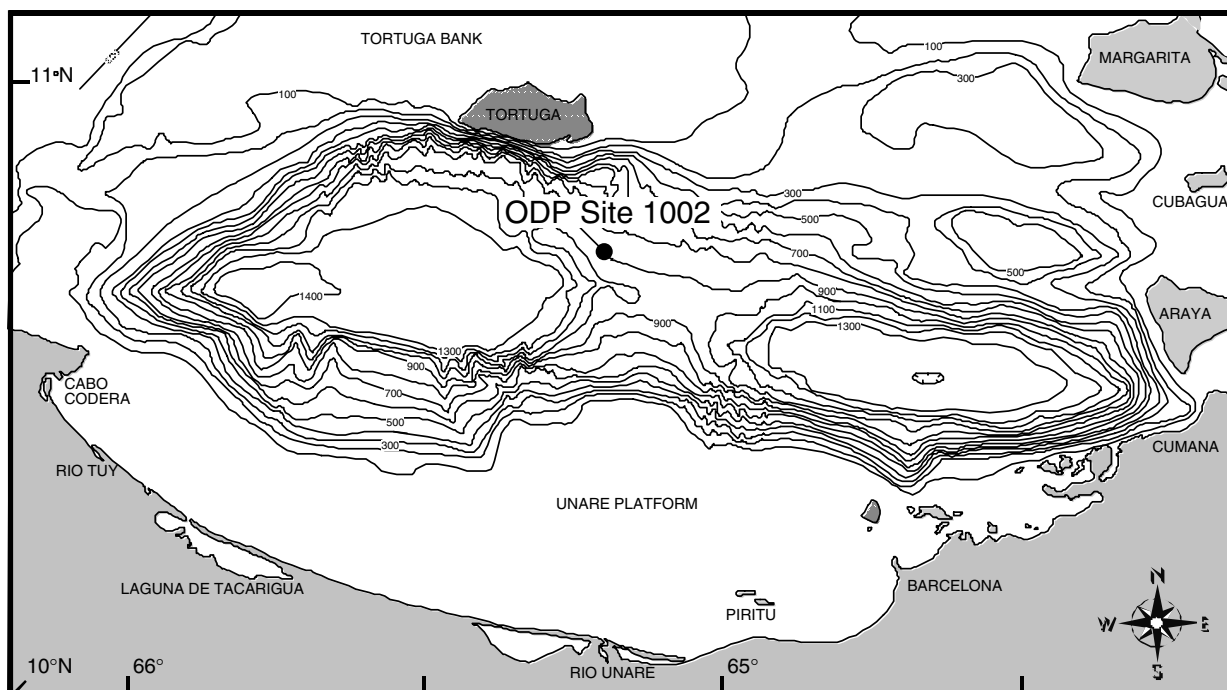


Fig. 1. Map and bathymetry of the Cariaco Basin, and the location of Site 1002, Ocean Drilling Program (ODP) Leg 165 (taken from Werne et al., 2003).

2.2.1. Sulfate profiles and steady-state solution

Concentration and isotopic composition data (Werne et al., 2003; Fig. 2) were used to generate concentration profiles for $^{32}\text{SO}_4^{2-}$ and $^{34}\text{SO}_4^{2-}$ (Fig. 3), according to equations

$$^{32}\text{SO}_4^{2-} = \text{TotalSO}_4^{2-} / (1 + \gamma(0.001 \cdot \delta^{34}\text{S} + 1)), \quad (4a)$$

and

$$^{34}\text{SO}_4^{2-} = \text{TotalSO}_4^{2-} / \left(1 + \frac{1}{\gamma(0.001 \cdot \delta^{34}\text{S} + 1)} \right), \quad (4b)$$

where $\gamma = 0.00450045$ is the standard isotopic ratio of $^{34}\text{S}/^{32}\text{S}$ in Vienna Canyon Diablo Troilite. The profiles so obtained were fit to give a depth-dependent concentration

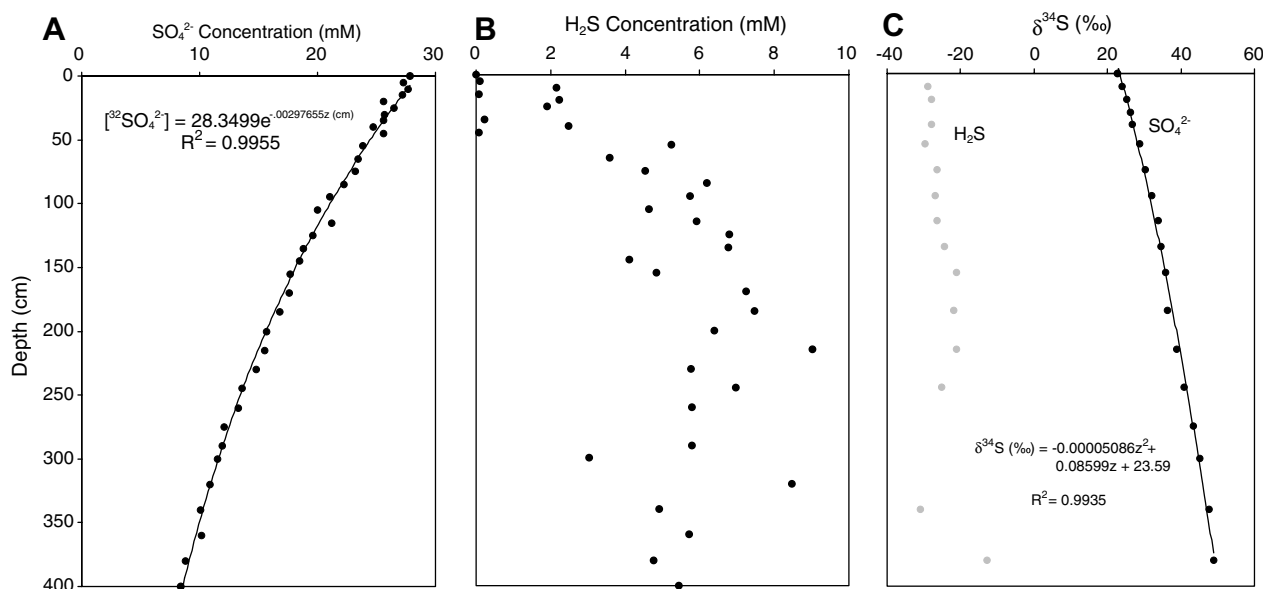


Fig. 2. Depth profiles of (A) SO_4^{2-} concentration (B) H_2S concentration, and (C) sulfur isotope composition of SO_4^{2-} and H_2S from the Cariaco Basin ODP Leg 165, Hole 1002B. Data from Werne et al. (2003).

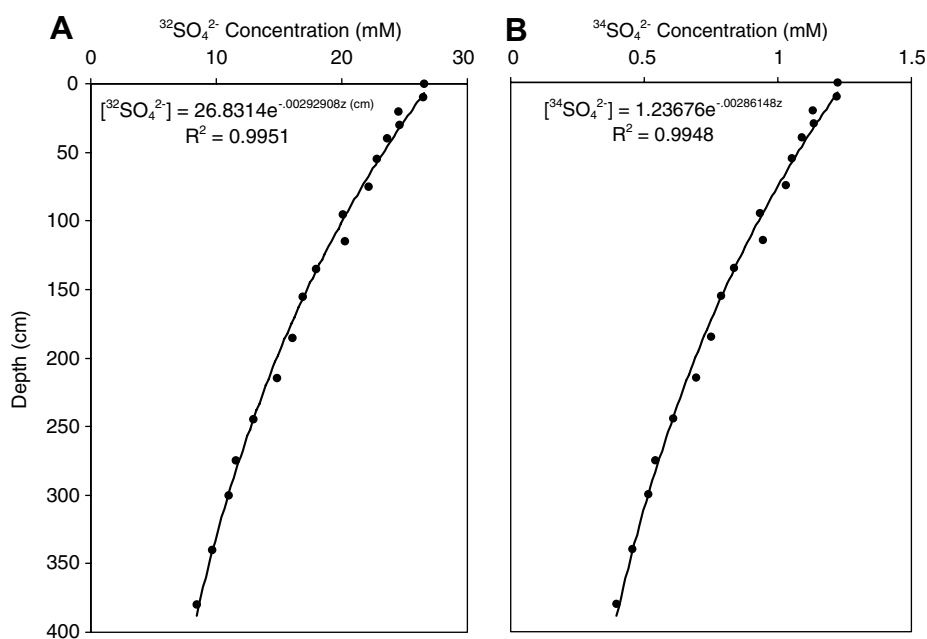


Fig. 3. Concentration profiles of (A) $^{32}\text{SO}_4^{2-}$ and (B) $^{34}\text{SO}_4^{2-}$ calculated from sulfate concentration and isotopic data from the Cariaco Basin ODP Leg 165, Hole 1002B (Werne et al., 2003). Notice that the curve in (B) is similar to the one for $^{32}\text{SO}_4^{2-}$ except for the large change in magnitude of the concentration data.

for both $^{32}\text{SO}_4^{2-}$ and $^{34}\text{SO}_4^{2-}$ from which rates and fractionation factors were then derived. For an exponential fit:

$$[{}^i\text{SO}_4^{2-}] = A_i e^{b_i z}, \quad (5)$$

where $i = 32$ or 34 . Substitution of Eq. (5) into Eq. (3) gives the individual net microbial sulfate reduction rates, $f(z)_i$, for $^{32}\text{SO}_4^{2-}$ and $^{34}\text{SO}_4^{2-}$, respectively, as shown below.

$$f(z)_i = -\frac{\partial}{\partial z} \cdot \left(D_{\text{sed}({}^i\text{SO}_4^{2-})} \phi \frac{\partial}{\partial z} [{}^i\text{SO}_4^{2-}] \right) + \frac{\partial}{\partial z} (\omega \phi [{}^i\text{SO}_4^{2-}]), \quad (6)$$

where the porosity term ϕ converts rates from per volume of pore water to per total volume of sediment. These rates were then summed to give the overall depth-dependent net rate of microbial sulfate reduction:

$$SR = f(z)_{32} + f(z)_{34}. \quad (7)$$

The net fractionation (ε_{SR}) is calculated as:

$$\varepsilon_{\text{SR}}(\text{‰}) = 1000 \cdot \left(\frac{R_{\text{red}}}{R_{\text{pw}}} - 1 \right), \quad (8)$$

where R_{pw} is the ratio of $[{}^{34}\text{SO}_4^{2-}]/[{}^{32}\text{SO}_4^{2-}]$ in pore water calculated from the fitted profiles (e.g., Eq. (5)), and the depth-dependent isotope ratio of the sulfate being reduced (R_{red}) is given by the ratio $f(z)_{34}/f(z)_{32}$ (determined using Eq. (6)).

2.2.2. Model parameters

In addition to the concentration profiles, the quantification of SR and ε_{SR} requires sediment porosity, sedimentation rate, sediment (bottom water) temperature, and the whole sediment diffusion coefficients for $^{32}\text{SO}_4^{2-}$ and $^{34}\text{SO}_4^{2-}$.

A porosity profile (Fig. 4) was obtained by converting Gamma Ray Attenuation Porosity Evaluation (GRAPE) raw data from piston core 1002B using standard methods outlined by the Deep Sea Drilling Project (Boyce, 1976). Porosity determinations were made at an interval of 2 cm for the entire length of the core. The model results were computed in two ways: (1) assuming a constant porosity equal to the average porosity over the 4 m interval, (2) using an empirical exponential fit to account for porosity changes with depth typically described as $\phi = \phi_{\infty} + (\phi_0 - \phi_{\infty})e^{-2x}$ (e.g., Murray et al., 1978).

Age control for core 1002B was provided by a suite of accelerator mass spectrometer (AMS) dates on individual planktonic foraminifera from core PL07-39PC (Lin et al., 1997). Core 1002B was correlated to PL07-39PC using high-resolution records of magnetic susceptibility (Werne et al., 2000), and sediment accumulation rates were subsequently determined from the age model. It is well documented that a dramatic shift in sedimentation rate occurred at ~ 11 ka (calendar years) with a change from ~ 100 cm/kyr prior to ~ 11 ka to ~ 30 cm/kyr since (Hughen et al., 1996; Werne et al., 2000). Consequently, the model considers only the first 4 m of core, and the average sedimentation rate used for the model was calculated to be 0.0359 cm/yr over the last 11,150 calendar years.

The whole sediment diffusion coefficient for $^{32}\text{SO}_4^{2-}$ was determined starting with the temperature-dependent rela-

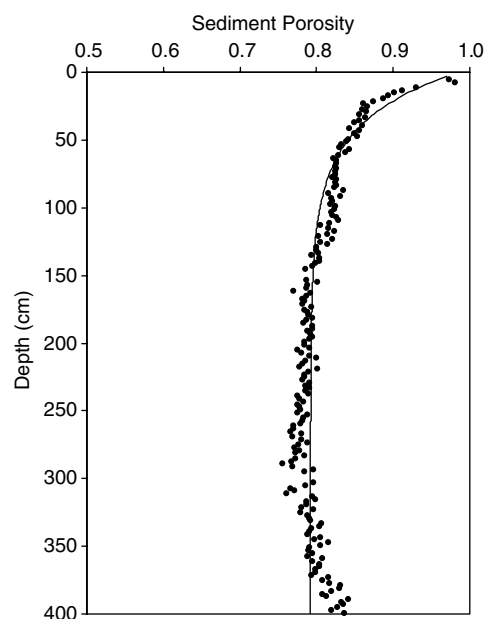


Fig. 4. Sediment porosity vs. depth obtained by converting Gamma Ray Attenuation Porosity Evaluation (GRAPE) raw data from piston core 1002B using standard methods outlined by the Deep Sea Drilling Project (Boyce, 1976). The solid black line is the empirical porosity fit used in the model.

tion for the diffusivity of sulfate in seawater as given by Schulz (2000):

$$D_{\text{sw}(\text{SO}_4^{2-})} = (4.655 + 0.2125T) \cdot 10^{-6} \text{ cm}^2/\text{s}, \quad (9)$$

where T is the temperature of the seawater in $^{\circ}\text{C}$. Recent measurements show temperatures that vary little within the anoxic zone of the Cariaco Basin from 400 to 1200 m depth (17.0–17.2 $^{\circ}\text{C}$ range, Muller-Karger et al., 2001); a sediment temperature of 17.1 $^{\circ}\text{C}$ was used. The diffusion coefficient for $^{32}\text{SO}_4^{2-}$ was computed using the following relation (Boudreau, 1997):

$$D_{\text{sed}} = \frac{D_{\text{sw}}}{(1 - 2 \ln \phi(z))}. \quad (10)$$

The isotope mass effect on the diffusion coefficient is taken into account as follows. The kinetic energy of a molecule i is given by:

$$kT = \frac{1}{2} m_i v_i^2, \quad (11)$$

where k is the Boltzmann constant, T is the absolute temperature, m is the mass, and v is the velocity of the molecule. Considering that the temperature experienced by a molecule of $^{32}\text{SO}_4^{2-}$ and a molecule of $^{34}\text{SO}_4^{2-}$ is equal, their respective kinetic energies must also be equal. Neglecting potential mass differences due to varying proportions of oxygen isotopes (see below), the mass difference ($m_{34\text{SO}_4^{2-}} = 96$), ($m_{32\text{SO}_4^{2-}} = 98$) leads to a slight difference in velocities, $v_{34\text{SO}_4^{2-}} = \sqrt{\frac{96}{98}} \cdot v_{32\text{SO}_4^{2-}}$. As a result, $^{32}\text{SO}_4^{2-}$ molecules should travel with a greater average velocity and diffuse faster than $^{34}\text{SO}_4^{2-}$ molecules, i.e.

$$D_{\text{sed}(^{34}\text{SO}_4^{2-})} = \sqrt{\frac{96}{98}} D_{\text{sed}(^{32}\text{SO}_4^{2-})}, \quad (12)$$

where $D_{\text{sed}(^{34}\text{SO}_4^{2-})}$ is estimated using Eq. (10).

3. RESULTS AND DISCUSSION

The calculated net microbial sulfate reduction rates are shown in Fig. 5, assuming a constant porosity of 0.81 and using the porosity fit described in Section 2.2.2 (Fig. 4). Using the porosity fit had a significant impact on the computed sulfate reduction rate in the upper 100 cm, causing as much as a five-fold increase near the surface when compared to the computed rate assuming a constant porosity (Fig. 5). However, in both cases the computed rate is extremely low ($<1 \text{ nmol cm}^{-3} \text{ d}^{-1}$). The sulfur isotope fractionation associated with microbial sulfate reduction in the Cariaco sediments for the two porosity fits is shown in Fig. 6. Using exponential fits to the $[^{32}\text{SO}_4^{2-}]$ and $[^{34}\text{SO}_4^{2-}]$ profiles (Eq. (5); Fig. 3) results in a constant fractionation of 53.4‰ for constant porosity. Including a fit to the porosity measurements (Fig. 4) leads to a lower fractionation of 36‰ near the sediment surface, which increases with depth until a constant value of about 53‰ is reached at about 2 m depth (Fig. 6).

To identify the impact of differences in diffusion coefficients on fractionation estimates, the diffusion coefficient for $^{34}\text{SO}_4^{2-}$ was varied. When the diffusion coefficient of $^{34}\text{SO}_4^{2-}$ was assumed to be equal to that of $^{32}\text{SO}_4^{2-}$, a large decrease of more than 9‰ was observed in ϵ_{SR} (Fig. 7),

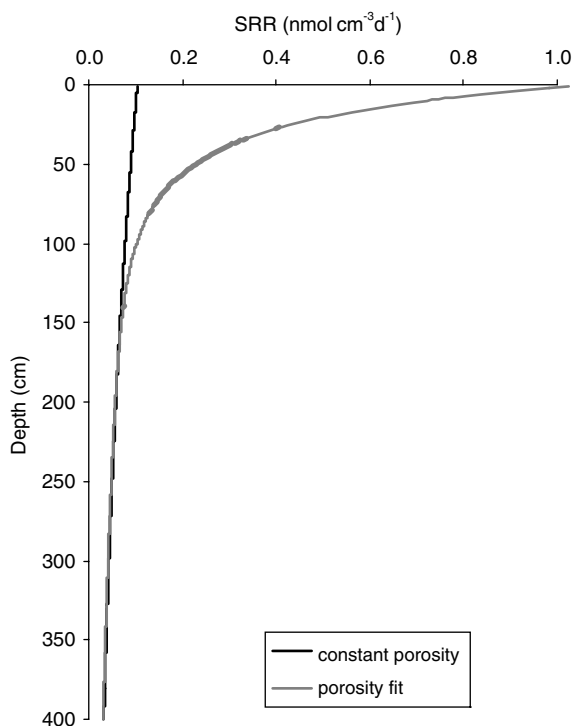


Fig. 5. Computed sulfate reduction rate vs. depth assuming a constant porosity (black) and using the empirical porosity fit in Fig. 4 (gray). Note that positive values here indicate the rate at which sulfate is removed via SR.

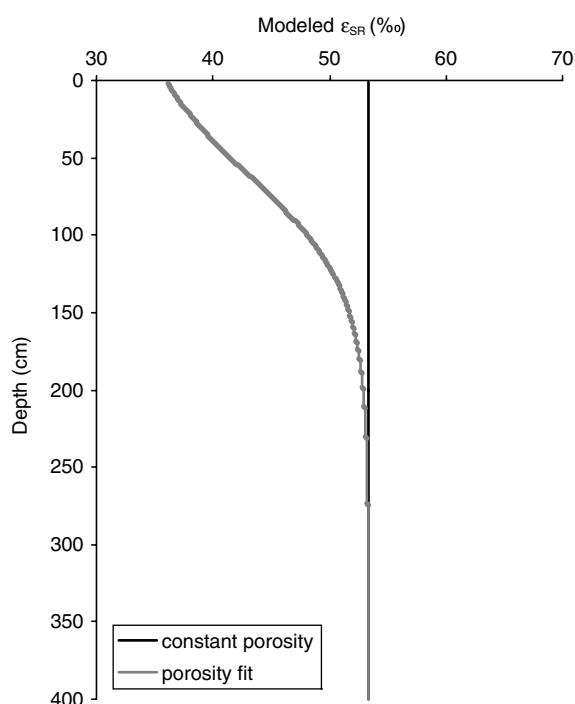


Fig. 6. Depth profile of modeled sulfur isotope fractionation associated with sulfate reduction assuming a constant porosity (black) and taking into account changes in porosity with depth (gray).

independent of the magnitude of the fractionation and the porosity fit used.

Environmental parameters were varied within ranges representative of Cariaco sediments to test for the relative influence of each on the steady-state solutions for the SR rate and associated sulfur isotope fractionation. Temperature was varied by $\pm 1 \text{ }^\circ\text{C}$ and sedimentation rate by $\pm 5 \text{ cm}/1000 \text{ yrs}$. Calculated sulfate reduction rates [Eq. (6)] depend mostly on the molecular diffusion coefficients whose values are constrained within a few percent, but show little sensitivity towards minor variations in temperature and sedimentation rate (not shown). In the cases where temperature was varied, the small changes in the computed rates of sulfate reduction ($<5\%$ in all cases) were due to the temperature dependence of diffusion. Similarly, the modeled fractionation changed very little ($<1\%$) when sedimentation rate and temperature were systematically varied (not shown).

3.1. Factors affecting sulfur isotope fractionation

The modeled fractionation exceeds values typically reported from cultures (cf Canfield, 2001b, and refs therein) but still lies within the theoretical maximum fractionation of more than 70‰ (Kaplan and Rittenberg, 1964; Brunner and Bernasconi, 2005). Beyond differences in the diffusion coefficients (Section 3.2), there are several possible factors that could be expected to contribute to a high ϵ_{SR} , including low cell specific rates of SR (Kaplan and Rittenberg, 1964; Chambers et al., 1975; Habicht and Canfield, 1997),

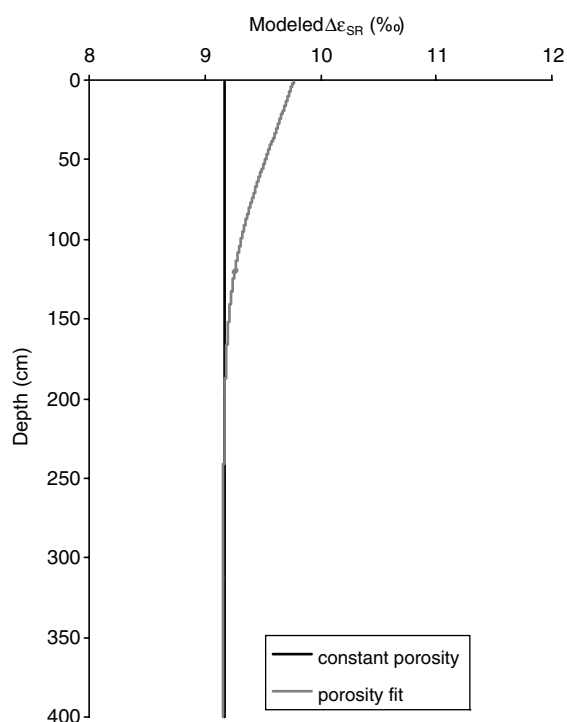


Fig. 7. Differences in ϵ_{SR} ($\Delta\epsilon$) due to the difference in the diffusion coefficients of the different isotopes. $\Delta\epsilon$ is the difference in fractionation factors obtained when assuming one generic diffusion coefficient ($D^{34}\text{SO}_4^{2-} = D^{32}\text{SO}_4^{2-}$) versus when taking into account the isotopic mass difference, $\alpha(D^{32}\text{SO}_4^{2-}$ and $D^{34}\text{SO}_4^{2-}$). Model values are shown both assuming a constant porosity (black) and accounting for variations in porosity with depth (gray).

growth-limiting sulfate concentrations (Canfield, 2001b), variations in temperature (Canfield et al., 2006), and the species of sulfate reducer (Canfield, 2001a; Brüchert, 2004 and references therein). As discussed above, sulfate concentrations (Fig. 2) exceed 8 mM, which is much greater than sulfate levels that have been shown to cause a diminished fractionation (Harrison and Thode, 1958; Canfield et al., 2000; Canfield, 2001b). Temperature is also expected to be approximately constant over the studied depth interval, which is characterized by a uniformly laminated sediment composition deposited under consistently anoxic conditions (Wakeham, 1990; Peterson et al., 1991).

In the absence of any direct measurements we cannot rule out variations in the community composition of sulfate-reducers, but the most distinct characteristic of the Cariaco Basin sediment is a net sulfate reduction rate ($<1 \text{ nmol cm}^{-3} \text{ d}^{-1}$) that is much lower than typically reported in marine environments (on the order of tens of $\text{nmol cm}^{-3} \text{ d}^{-1}$ to $\mu\text{mol cm}^{-3} \text{ d}^{-1}$; Habicht and Canfield, 1997; Hurtgen et al., 1999; Rudnicki et al., 2001; Weber et al., 2001; Brüchert et al., 2003). The rate calculated in this study is a net rate; however, the oxidative recycling of sulfide is not expected to influence the SR rate due to the presence of anoxic/sulfidic conditions (Canfield, 2001a) and the low abundance of oxidants such as Fe_2O_3 , MnO_2 and NO_3^- (Lyons et al., 2003). In addition, underestimation

of the reduction rate due to enhanced sulfate transport via bioirrigation can be ruled out because of anoxic conditions (cf. Werne et al., 2003). As a result, the gross rate is not likely to be appreciably different from the calculated net microbial sulfate reduction rate in the Cariaco Basin, and the low computed value is likely to be a suitable approximation of the *in situ* SR rate. Although no significant correlation is typically observed between the volumetric (mass volume $^{-1}$ time $^{-1}$) or cell-specific (mass cell $^{-1}$ time $^{-1}$) sulfate reduction rate and ϵ_{SR} (Detmers et al., 2001), the largest fractionations during microbial sulfate reduction are often associated with the lowest rates of volumetric sulfate reduction (Habicht and Canfield, 1997), and at least one recent study has identified a clear relationship between low sulfate reduction rate and greater fractionation (Hoek et al., 2006). At present, we are unable to make concrete conclusions on the basis of cell specific sulfate reduction rates; however, the results here echo findings in other studies (Rudnicki et al., 2001; Böttcher et al., 2004) in which anomalously high fractionations are associated with volumetric microbial sulfate reduction rates that are extremely low, on the order of 2–45 $\text{pmoles cm}^{-3} \text{ d}^{-1}$, though it should be noted that in at least one case, high fractionations were associated with sulfate reduction rates on the order of 25 $\text{nmol cm}^{-3} \text{ d}^{-1}$ (Wortmann et al., 2001).

3.2. Influence of diffusion coefficients on modeled fractionation

Previous studies (Jørgensen, 1979; Fossing et al., 2000; Jørgensen et al., 2004) have assumed equal values for the diffusion coefficients for ^{32}S and ^{34}S pore water constituents. In contrast, the present model considers isotopic mass differences for the sulfate diffusion coefficients. Our results indicate that ϵ_{SR} is strongly dependent on the ratio of whole sediment diffusion coefficients used for $^{32}\text{SO}_4^{2-}$ and $^{34}\text{SO}_4^{2-}$, with a difference of nearly 10‰ attributed to the assumption of unique diffusion coefficients for $^{32}\text{SO}_4^{2-}$ and $^{34}\text{SO}_4^{2-}$ based on their molecular mass. These results are in agreement with a recent study that demonstrated that the diffusion coefficients of H_2^{32}S and H_2^{34}S differ (Piel, 1999). These studies indicate the need for further experimentation to better constrain sulfate diffusion coefficients.

Note that the impact of the difference in diffusion coefficients is fairly independent of the fitting approach, yielding results that vary between 9‰ and 10‰ (Fig. 7), illustrating that this is a robust finding. The impact on ϵ_{SR} is due to changes in the proportion of transport due to diffusion and advection due to sedimentation. If diffusion were responsible for all of the transport, the difference in fractionation would simply be equal to the difference between the two diffusion coefficients determined using Eq. (12) (1.03% = 10.3‰).

3.3. Impact of model structure and uncertainty analysis

Apart from being affected by environmental conditions, cell specific rates and mass-dependent diffusion coefficients, model estimates are biased by the model structure used to interpret the data. Including a fit to the porosity

measurements in the analysis of the $^{32}\text{SO}_4^{2-}$ and $^{34}\text{SO}_4^{2-}$ profiles leads to a near surface fractionation of 36‰, which increases with depth until a constant value of 53‰ is reached at about 2 m depth (Fig. 6).

The somewhat arbitrary choice of fitting functions affects the estimates of absolute values of ε_{SR} . The impact of uncertainties associated with the data fitting procedure can be analyzed through error propagation, and the effect of the uncertainty in parameter $p(s_p)$ on ε_{BSR} can be expressed as:

$$s_\varepsilon^2 = \sum_i \left(\left(\frac{\partial \varepsilon}{\partial p_i} \right)^2 s_i^2 \right) + 2 \sum_{j \neq i} \frac{\partial \varepsilon}{\partial p_i} \frac{\partial \varepsilon}{\partial p_j} s_{ij}, \quad (13)$$

where parameter variances (s_i^2) and covariances (s_{ij}) were determined using MATLAB's nonlinear least-squares regression fitting the concentration and porosity profiles, respectively. For example, when combining an exponential fit for total sulfate and a 2nd order polynomial approximation to the $\delta^{34}\text{S}$ data ($R^2 > 0.994$ for both) with the above variable porosity fit, ε_{SR} ranges from about -63% to -44% , with a 95% confidence interval on the order of $<3\%$ (not shown). Notably, the sulfate reduction rate profile via Eq. (6) is sensitive to the choice of the fitting function (Fig. 5), particularly in the uppermost 50 cm. Thus, direct rate measurements, while currently not available in this system, could be used to further corroborate the high fractionation values.

3.4. Reconciling the observed sulfate-sulfide isotopic offset with the modeled fractionation

An isotopic offset ($\Delta\delta^{34}\text{S}_{\text{SO}_4\text{-H}_2\text{S}}$) between pore water sulfate and sulfide of 45–70‰ is often observed in sedimentary environments (Canfield and Thamdrup, 1994), and is also detected in the Cariaco Basin, where values generally increase from $\sim 53\%$ near the sediment water interface to $\sim 60\text{--}63\%$ at 4 m depth (Fig. 4, data from Werne et al., 2003). Several previous studies have explained such observed trends in $\Delta\delta^{34}\text{S}_{\text{SO}_4\text{-H}_2\text{S}}$ through repeated cycles of sulfide oxidation followed by disproportionation of intermediate species such as elemental sulfur, leading to sulfide that is progressively depleted in ^{34}S (Canfield and Thamdrup, 1994; Habicht and Canfield, 1997; Sørensen and Canfield, 2004). However, in the Cariaco Basin bacterial disproportionation is an unlikely explanation for the measured offset, because bacteria that have been shown to disproportionate elemental sulfur become inactive in the presence of sulfide at concentrations >1 mM (Thamdrup et al., 1993), and pore water sulfide concentrations in Core 1002B are substantially greater than 1 mM at all depths below 50 cm (Fig. 2). Furthermore, before disproportionation can occur, the sulfide must be oxidized to intermediate sulfur forms, and in the Cariaco Basin sediments, there is a lack of available oxidants. Previous studies have measured reactive iron using both the HCl and dithionite extractions and found that, though iron sulfides do continue to form with depth in the Cariaco, the concentrations of residual 'reactive' Fe species are very low and are likely composed of silicate iron that is reactive only on timescales of 10^3 to

10^5 years (Canfield et al., 1992; Raiswell and Canfield, 1998; Lyons et al., 2003; Werne et al., 2003). Thus, while the reaction of sulfide with iron silicates on long time scales (Canfield et al., 1992) cannot be discounted, it is likely a small sink for pore water sulfide produced by microbial SR, and the amounts are thought to be negligible (Lyons et al., 2003). It is also possible that the pore water sulfide could be oxidized by reaction with dissolved organic matter (DOM; Heitmann and Blodau, 2006), though at this point we cannot quantify this as no measurements of DOM have been made in Cariaco sediment pore waters. Thus, while there are some possible oxidants for reaction with sulfide, they are either documented to be small (e.g., Fe, see Lyons et al., 2003) or presently undocumented (DOM). As a result, the authors assume negligible oxidative sulfur cycling in the Cariaco Basin sediments.

Another explanation for a high isotopic offset in a sulfidic environment is that oxidative cycling (including disproportionation) is occurring only near the sediment-water interface where sulfide is not abundant, leading to a large offset in the near surface sediments that is propagated downward as sedimentation continues (Böttcher et al., 2004). This explanation is also unsatisfactory in the Cariaco Basin because the steady state solution for the fractionation requires a high fractionation at all depths including the region below 50 cm, where sulfide concentrations exceed 1 mM (Werne et al., 2003).

The present study suggests that high fractionation (possibly associated with the low sulfate reduction rate) coupled with diffusive transport is a viable alternative explanation for the observed isotopic offset ($\Delta\delta^{34}\text{S}_{\text{SO}_4\text{-H}_2\text{S}}$) that gets larger with increasing depth in the sediments. Our model results indicate that, by including the effects of differential diffusion coefficients, the instantaneous $\Delta\delta^{34}\text{S}_{\text{SO}_4\text{-H}_2\text{S}}$ (i.e., epsilon) will be 53.4‰ at the depth of maximum sulfide concentration (~ 200 cm). S isotope data (from Werne et al., 2003; Fig. 2) show a $\Delta\delta^{34}\text{S}_{\text{SO}_4\text{-H}_2\text{S}}$ of approximately 58‰ near 200 cm depth, which is greater than our model results, though given the uncertainty of the model structure, it is within the error of our calculations on the absolute fractionation value. Combined with the error inherent in the analyses of pore water sulfide (cf Werne et al., 2003), we consider the difference in these values insignificant at the depth of maximum sulfide concentration.

Below 200 cm, however, the measured $\Delta\delta^{34}\text{S}_{\text{SO}_4\text{-H}_2\text{S}}$ continues to increase with depth in the sediments to values considerably greater than our modeled results of $\sim 53\%$. This observation can be explained by considering the effects of differential diffusion of the isotopologues of sulfate ($^{32}\text{SO}_4^{2-}$ and $^{34}\text{SO}_4^{2-}$) relative to those of sulfide (H_2^{32}S and H_2^{34}S). Due to the steady decrease in concentrations with depth, both $^{32}\text{SO}_4^{2-}$ and $^{34}\text{SO}_4^{2-}$ are diffusing downward. Because the $^{32}\text{SO}_4$ is preferentially reduced to sulfide pore water sulfate at any given depth is ^{34}S enriched relative to that above it, but this progressive ^{34}S enrichment is slightly moderated by the fact that $^{32}\text{SO}_4$ diffuses into the sediment slightly faster than $^{34}\text{SO}_4$, based on its smaller molecular mass and steeper normalized gradient, when gradients are normalized for variations in concentration

(Goldhaber and Kaplan, 1980; Chanton et al., 1987; Jørgensen et al., 2004).

In contrast, sulfide diffuses both upwards and downwards away from the zone of maximum production (via sulfate reduction), at approximately 200 cm depth in the Cariaco Basin sediments. As with sulfate, for a constant fractionation factor, at any given depth, the *in situ* produced sulfide is ^{34}S enriched relative to that above it. Thus, above the depth of maximum sulfide production, the upward diffusing sulfide is ^{34}S enriched relative to *in situ* produced sulfide because of the ^{34}S enriched sulfate source (compared to shallower depths); however because H_2^{32}S diffuses faster than H_2^{34}S , this ^{34}S enrichment is minimized, and the upward diffusing sulfide has little net impact on the $\delta^{34}\text{S}$ in shallow sediments.

In contrast, below the depth of maximum sulfide concentration, the aqueous sulfide present is a combination of sulfide formed *in situ* (^{34}S depleted relative to that below it) and sulfide diffusing downwards (^{34}S depleted due to more rapid diffusion of H_2^{32}S). As a result, below the subsurface maximum we would expect the isotopic trend toward more enriched sulfide to increase less rapidly compared to the isotopic trend in sulfate. The net effect of these diffusive isotopic effects is that $\Delta\delta^{34}\text{S}_{\text{SO}_4\text{-H}_2\text{S}}$ will continue to increase with increasing depth. It is important to note that this mechanism can account for offsets much larger than observed fractionations. This mechanism has important implications for deeper cores, where it may be possible to account for offsets as large as 100‰ or greater, provided that sulfide is transported downward over a significant distance.

4. CONCLUSIONS

Modeling of data from the Cariaco Basin resulted in an extremely high ϵ_{SR} associated with microbial sulfate reduction. The dependence of the calculated fractionation on the ratio of whole sediment diffusion coefficients for $^{32}\text{SO}_4^{2-}$ and $^{34}\text{SO}_4^{2-}$ used in the model demonstrates the necessity for carefully designed experiments to evaluate the precise molecular diffusion coefficients for $^{32}\text{SO}_4^{2-}$ and $^{34}\text{SO}_4^{2-}$ in sedimentary environments. Additionally, in light of other recent studies (Rudnicki et al., 2001; Böttcher et al., 2004), it seems likely that the large fractionation reported here could result from low cell specific sulfate reduction rates; however, this cannot be confirmed without direct rate measurements, and other possibilities can therefore not be ruled out.

Measured data from the Cariaco Basin (Fig. 2) indicate a large offset between pore water sulfate and sulfide, similar in magnitude to values observed in many other anoxic environments. This study suggests that open system diffusion, coupled with a high fractionation, rather than bacterial disproportionation, can lead to an offset larger in magnitude than the computed fractionation. Our findings emphasize the necessity to take into account differences in diffusion coefficients of different isotopes in the context of isotope fractionation. Typical fractionations observed in marine sediments, including both oxic and anoxic settings, are on the order of 0–50‰ such that even a small potential difference in diffusion coefficients (1%) can have a significant impact on isotopic data and their interpretation.

The observed isotopic offset between sedimentary sulfides and oceanic sulfate has been used as a proxy for the fractionation imparted during ancient sulfate reduction, and to infer the timing of major changes in the oxidation state of the early earth (Canfield, 1998; Canfield et al., 2000; Shen et al., 2001; Hurtgen et al., 2005; Fike et al., 2006). Specifically, the emergence of an offset larger than 4‰ around 2.20–2.30 Ga has been interpreted as evidence of bacterial sulfate reduction under non-limiting sulfate (>1 mM), implying a larger concentration of global oceanic sulfate, which in turn provides evidence for an oxidation event around that time (Farquhar and Wing, 2003). Perhaps even more significant is the increase in the $\Delta\delta^{34}\text{S}_{\text{SO}_4\text{-H}_2\text{S}}$ occurring in the Neoproterozoic (~600 Ma) that has been interpreted as evidence of the onset of the oxidative side of the sulfur cycle (including sulfide oxidation and disproportionation; Canfield and Teske, 1996; Canfield, 1998). While this interpretation is debated (cf Hurtgen et al., 2005; Johnston et al., 2005; Philippot et al., 2007), our results suggest that the larger offsets observed after ~600 Ma may be related in part to diffusive effects rather than to the onset of sulfide oxidation and disproportionation. Thus, if differential rates of diffusion for $^{32}\text{SO}_4^{2-}$ and $^{34}\text{SO}_4^{2-}$ are impacting the actual oceanic $\Delta\delta^{34}\text{S}_{\text{SO}_4\text{-H}_2\text{S}}$, then the signal being preserved in sedimentary sulfate and sulfide minerals does not reflect the actual fractionation imparted during sulfate reduction. As a result, the authors caution against using this offset as an indicator of sulfur isotope fractionation imparted in ancient systems. Furthermore, interpretations of atmospheric and oceanic chemical evolution should be re-evaluated within the context of these results to ascertain that they remain valid.

ACKNOWLEDGMENTS

The authors gratefully acknowledge the contributions of Harlan Stech, whose discussions in early phases of this research were invaluable. Comments by the Associate Editor M. Goldhaber and reviews by B. Brunner, B.B. Jørgensen, and an anonymous reviewer helped to significantly improve the manuscript. This research was supported in part by a University of Minnesota Grant-in-Aid of Research to J.P.W. and the U.S. National Science Foundation to T.L. C.M. and T.L. acknowledge fellowships that provided financial support and hospitality at the Hanse Institute for Advanced Study in Delmenhorst, Germany.

REFERENCES

- Berner R. A. (1964) An idealized model of dissolved sulfate distribution in recent sediments. *Geochim. Cosmochim. Acta* **28**, 1497–1503.
- Berner R. A. (1982) Burial of organic carbon and pyrite sulfur in the modern ocean: its geochemical and environmental significance. *Am. J. Sci.* **282**, 451–473.
- Berner R. A. (1984) Sedimentary pyrite formation: an update. *Geochim. Cosmochim. Acta* **48**, 605–615.
- Berner R. A. and Petsch S. T. (1998) The sulfur cycle and atmospheric oxygen. *Science* **282**, 1426–1427.
- Böttcher M. E., Boo-Kuen K., Suzuki A., Gehre M., Wortmann U. G. and Brumsack H. J. (2004) Microbial sulfate reduction in deep sediments of the Southwest Pacific (ODP Leg 181, Sites 1119–1125): evidence from stable sulfur isotope fractionation and pore water modeling. *Mar. Geol.* **205**, 249–260.

- Bottrell S. H. and Raiswell R. (2000) Sulphur isotopes and microbial sulphur cycling in microbial sediments (eds. R. E. Riding and S. M. Awramik). Springer-Verlag, Berlin, pp. 96–104.
- Boudreau B. P. (1997) *Diagenetic Models and Their Implementation: Modeling Transport and Reactions in Aquatic Sediments*. Springer-Verlag, Berlin, NY, pp. 414.
- Boyce, R. E. (1976) Leg 33, definitions and laboratory techniques of compressional sound velocity parameters and wet-water content, wet-bulk density, and porosity parameters by gravimetric and gamma attenuation techniques. In *Init. Rep. DSDP* (eds. S. O. Schlanger and E. D. Jackson, et al.). pp. 931–958.
- Brüchert, V. (2004) Physiological and ecological aspects of sulfur isotope fractionation during bacterial sulfate reduction. In *Sulfur Biogeochemistry—Past and Present* (eds. J. P. Amend, K. J. Edwards and T. W. Lyons). GSA Special Paper 379, pp. 1–16.
- Brüchert V., Jørgensen B., Neumann K., Riechmann D., Schlösser M. and Schulz H. (2003) Regulation of bacterial sulfate reduction and hydrogen sulfide fluxes in the central Namibian coastal upwelling zone. *Geochim. Cosmochim. Acta* **67**, 4505–4518.
- Brunner B. and Bernasconi S. M. (2005) A revised isotope fractionation model for dissimilatory sulfate reduction in sulfate reducing bacteria. *Geochim. Cosmochim. Acta* **69**, 4759–4771.
- Canfield D. E. (1998) A new model for Proterozoic ocean chemistry. *Nature* **396**, 450–453.
- Canfield D. E., Habicht K. S. and Thamdrup B. (2000) The Archean sulfur cycle and early history of atmospheric oxygen. *Science* **288**, 658–661.
- Canfield D. E. (2001a) Biogeochemistry of sulfur isotopes. In *Stable Isotope Geochemistry*, vol. 43 (eds. J. W. Valley and D. R. Cole), pp. 607–636. Reviews in Mineralogy and Geochemistry. Mineralogical Society of America and Geochemical Society.
- Canfield D. E. (2001b) Isotope fractionation by natural populations of sulfate-reducing bacteria. *Geochim. Cosmochim. Acta* **65**, 1117–1124.
- Canfield D. E. and Thamdrup B. (1994) The production of ^{34}S -depleted sulfide during bacterial disproportionation. *Science* **266**, 1973–1975.
- Canfield D. E. and Teske A. (1996) Late Proterozoic rise in atmospheric oxygen concentration inferred from phylogenetic and sulphur-isotope studies. *Nature* **382**, 127–132.
- Canfield D. E., Raiswell R. and Bottrell S. (1992) The reactivity of sedimentary iron minerals toward sulfide. *Am. J. Sci.* **292**, 818–834.
- Canfield D. E., Jørgensen B. B., Fossing H., Glud R., Gundersen N. B., Ramsing B., Thamdrup B., Hansen J. W., Nielsen L. P. and Hall P. O. J. (1993) Pathways of organic carbon oxidation in three continental margin sediments. *Mar. Geol.* **113**, 27–40.
- Canfield D. E., Olesen C. A. and Cox R. P. (2006) Temperature and its control of isotope fractionation by a sulfate-reducing bacterium. *Geochim. Cosmochim. Acta* **70**, 548–561.
- Chambers L. A., Trudinger P. A., Smith J. W. and Burns M. S. (1975) Fractionation of sulfur isotopes by continuous cultures of *Desulfivibrio desulfuricans*. *Can. J. Microbiol.* **21**, 1602–1607.
- Chanton J. P., Martens C. S. and Goldhaber M. B. (1987) Biogeochemical cycling in an organic-rich coastal marine basin: a sulfur isotopic budget balanced by differential diffusion across the sediment–water interface. *Geochim. Cosmochim. Acta* **51**, 1201–1208.
- Detmers J., Brüchert V., Habicht K. S. and Kuever J. (2001) Diversity of sulfur isotope fractionations by sulfate-reducing prokaryotes. *Appl. Environ. Microbiol.* **67**, 888–894.
- Farquhar J. and Wing B. (2003) Multiple sulfur isotopes and the evolution of the atmosphere. *Earth Planet. Sci. Lett.* **213**, 1–13.
- Fike D. A., Grotzinger J. P., Pratt L. M. and Summons R. E. (2006) Oxidation of the Ediacaran ocean. *Nature* **444**, 744–747.
- Fossing H. and Jørgensen B. B. (1990) Oxidation and reduction of radiolabeled inorganic sulfur compounds in an estuarine sediment, Kysing Fjord, Denmark. *Geochim. Cosmochim. Acta* **54**, 2731–2742.
- Fossing H., Ferdelman T. G. and Berg P. (2000) Sulfate reduction and methane oxidation in continental margin sediments influenced by irrigation (South-East Atlantic off Namibia). *Geochim. Cosmochim. Acta* **64**, 897–910.
- Garrels R. M. and Lerman A. (1984) Coupling of the sedimentary sulfur and carbon cycles—an improved model. *Am. J. Sci.* **284**, 989–1007.
- Goldhaber M. B. and Kaplan I. R. (1980) Mechanisms of sulfur incorporation and isotope fractionation during early diagenesis in sediments of the Gulf of California. *Mar. Chem.* **9**, 95–143.
- Habicht K. S. and Canfield D. E. (1997) Sulfur isotope fractionation during bacterial sulfate reduction in organic-rich sediments. *Geochim. Cosmochim. Acta* **61**, 5351–5361.
- Habicht K. S., Canfield D. E. and Rethmeier J. (1998) Sulfur isotope fractionation during bacterial reduction and disproportionation of thiosulfate and sulfite. *Geochim. Cosmochim. Acta* **62**, 2585–2595.
- Habicht K. S., Gade M., Thamdrup B., Berg P. and Canfield D. E. (2002) Calibration of sulfate levels in the Archaean ocean. *Science* **282**, 2372–2374.
- Habicht K. S., Salling L., Thamdrup B. and Canfield D. E. (2005) Effect of low sulfate concentrations on lactate oxidation and isotope fractionation during sulfate reduction by *Archaeoglobus fulgidus* Strain Z. *App. Environ. Microbiol.* **71**, 3770–3777.
- Harrison A. G. and Thode H. G. (1958) Mechanism of the bacterial reduction of sulphate from isotope fractionation studies. *Trans. Faraday Soc.* **54**, 84–92.
- Heitmann T. and Blodau C. (2006) Oxidation and incorporation of hydrogen sulfide by dissolved organic matter. *Chem. Geol.* **235**, 12–20.
- Hoek J., Reysenbach A., Habicht K. and Canfield D. (2006) Effect of hydrogen limitation and temperature on the fractionation of sulfur isotopes by a deep-sea hydrothermal vent sulfate-reducing bacterium. *Geochim. Cosmochim. Acta* **70**, 5831–5841.
- Holser W. and Kaplan I. R. (1966) Isotope geochemistry of sedimentary sulfates. *Chemical Geology* **1**, 1–17.
- Hughen K., Overpeck J. T., Peterson L. C. and Anderson R. F. (1996) The nature of varved sedimentation in the Cariaco Basin, Venezuela, and its palaeoclimatic significance. In *Palaeoclimatology and Palaeoceanography From Laminated Sediments* (ed. A. E. S. Kemp), vol. 116. Geol. Soc. Spec. Pub., pp. 171–183.
- Hurtgen M., Lyons T., Ingall I. and Cruse A. (1999) Anomalous enrichments of iron monosulfide in euxinic marine sediments and the role of H_2S in iron sulfide transformations: examples from Effingham Inlet, Orca Basin, and the Black Sea. *Am. J. Sci.* **299**, 556–588.
- Hurtgen M. T., Arthur M. A. and Halverson G. P. (2005) Neoproterozoic sulfur isotopes, the evolution of microbial sulfur species, and the burial efficiency of sulfide as sedimentary pyrite. *Geology* **33**, 41–44.
- Johnston D. T., Wing B. A., Farquhar J., Kaufman A. J., Strauss H., Lyons T. W., Kah L. C. and Canfield D. E. (2005) Active microbial sulfur disproportionation in the Mesoproterozoic. *Science* **310**, 1477–1479.
- Johnston D., Farquhar J. and Canfield D. (2007) Sulfur isotope insights into microbial sulfate reduction: When microbes meet models. *Geochim. Cosmochim. Acta* **71**, 3929–3947.

- Jørgensen B. B. (1979) A theoretical model of the stable sulfur isotope distribution in marine sediments. *Geochim. Cosmochim. Acta* **43**, 363–374.
- Jørgensen B. B. (1990a) The sulfur cycle of freshwater sediments: role of thiosulfate. *Limnol. Oceanogr.* **35**, 1329–1342.
- Jørgensen B. B. (1990b) A thiosulfate shunt in the sulfur cycle of marine sediments. *Science* **249**, 152–154.
- Jørgensen B. B., Böttcher M. E., Lüschen H., Neretin L. N. and Volkov I. I. (2004) Anaerobic methane oxidation and a deep H₂S sink generate isotopically heavy sulfides in Black Sea sediments. *Geochim. Cosmochim. Acta* **68**, 2095–2118.
- Kah L. C., Lyons T. W. and Frank T. D. (2004) Low marine sulphate and protracted oxygenation of the Proterozoic biosphere. *Nature* **431**, 834–838.
- Kaplan I. R. and Rittenberg S. C. (1964) Microbiological fractionation of sulfur isotopes. *J. Gen. Microbiol.* **34**, 195–212.
- Kemp A. L. W. and Thode H. G. (1968) The mechanism of the bacterial reduction of sulphate and sulphite from isotope fractionation studies. *Geochim. Cosmochim. Acta* **32**, 71–91.
- Lin H., Peterson L. C., Overpeck J. T., Trumbore S. E. and Murray D. W. (1997) Late Quaternary climate change from $\delta^{18}\text{O}$ records of multiple species of planktonic foraminifera: high-resolution records from the anoxic Cariaco Basin, Venezuela. *Paleoceanography* **12**, 415–427.
- Lyons T. W., Werne J. P., Hollander D. J. and Murray R. W. (2003) Contrasting sulfur geochemistry and Fe/Al and Mo/Al ratios across the last oxic-to-anoxic transition in the Cariaco Basin, Venezuela. *Chem. Geol.* **195**, 131–157.
- Muller-Karger F., Varela R., Thunell R., Scranton M., Bohrer R., Taylor G., Capelo J., Astor Y., Tappa E., Ho T. and Walsh J. (2001) Annual cycle of primary production in the Cariaco Basin: response to upwelling and implications for vertical export. *J. Geophys. Res.* **106**, 4527–4542.
- Murray J. W., Grundmanis V. and Smethie W. M. (1978) Interstitial water chemistry in the sediments of Saanich Inlet. *Geochim. Cosmochim. Acta* **42**, 1011–1026.
- Nakai N. and Jensen M. L. (1964) The kinetic isotope effect in the bacterial reduction and oxidation of sulphur. *Geochim. Cosmochim. Acta* **28**, 1893–1912.
- Paytan A., Kastner M., Campbell D. R. and Thiemens M. H. (1998) Sulfur isotopic composition of Cenozoic seawater sulfate. *Science* **282**, 1459–1462.
- Peterson L. C., Overpeck J. T., Kipp N. G. and Imbrie J. (1991) A high-resolution late quaternary upwelling record from the anoxic Cariaco Basin, Venezuela. *Paleoceanography* **6**, 99–119.
- Philippot P., Van Zuilen M., Lepot K., Thomazo C., Farquhar J. and Van Kranendonk M. J. (2007) Early Archaean microorganisms preferred elemental sulfur, not sulfate. *Science* **317**, 1534–1537.
- Piel C. (1999) Experimental Studies of Sulfur Isotope Fractionation (³⁴S/³²S) During Transport and Reaction of Dissolved and Gaseous Sulfur Species. M.Sc. Thesis, University of Bremen, Germany, 98 pp. (in German).
- Price F. T. and Shieh Y. N. (1979) Fractionation of sulfur isotopes during laboratory synthesis of pyrite at low temperatures. *Chem. Geol.* **27**, 245–253.
- Raiswell R. and Canfield D. E. (1998) Sources of iron for pyrite formation in marine sediments. *Am. J. Sci.* **298**, 219–245.
- Rees C. E. (1973) A steady state model for sulphur isotope fractionation in bacterial reduction processes. *Geochim. Cosmochim. Acta* **37**, 1141–1162.
- Rudnicki M. D., Elderfield H. and Spiro B. (2001) Fractionation of sulfur isotopes during bacterial sulfate reduction in deep ocean sediments at elevated temperatures. *Geochim. Cosmochim. Acta* **65**, 777–789.
- Schulz H. D. (2000) Quantification of early diagenesis: dissolved constituents in marine pore water. In *Marine Geochemistry* (eds. H. D. Schulz and M. Zabel). Springer, pp. 87–128.
- Shen Y. A., Buick R. and Canfield D. E. (2001) Isotope evidence for microbial sulphate reduction in the early Archean. *Nature* **410**, 77–81.
- Shipboard Scientific Party (1997) Site 1002, Proc. Ocean Drill. Program Init. Rep. 165, pp. 359–370.
- Sørensen K. B. and Canfield D. E. (2004) Annual fluctuations in sulfur isotope fractionation in the water column of a euxinic marine basin. *Geochim. Cosmochim. Acta* **68**, 503–515.
- Thamdrup B., Finster K., Hansen J. W. and Bak F. (1993) Bacterial disproportionation of elemental sulfur coupled to chemical reduction of iron and manganese. *Geol. Soc. Spec. Pub.* **59**, 101–108.
- Thode H. G. and Monster J. (1965) Sulfur-isotope geochemistry of petroleum, evaporates, and ancient seas. *Am. Assoc. Petrol. Geol. Mem.* **4**, 367–377.
- Wakeham S. (1990) Algal and bacterial hydrocarbons in particulate matter and interfacial sediment of the Cariaco Trench. *Geochim. Cosmochim. Acta* **54**, 1325–1336.
- Weber A., Riess W., Wenzhoefer F. and Jørgensen B. (2001) Sulfate reduction in Black Sea sediments: *in situ* and laboratory radiotracer measurements from the shelf to 2000 m depth. *Deep-Sea Res.* **1** **48**, 2073–2096.
- Werne J. P., Hollander D. J., Lyons T. W. and Peterson L. C. (2000) Climate-induced variations in productivity and planktonic ecosystem structure from the Younger Dryas to Holocene in the Cariaco Basin, Venezuela. *Paleoceanography* **15**(1), 19–29.
- Werne J. P., Lyons T. W., Hollander D. J., Formolo M. J. and Sinninghe Damsté J. S. (2003) Reduced sulfur in euxinic sediments of the Cariaco Basin: sulfur isotope constraints on organic sulfur formation. *Chem. Geol.* **195**, 159–179.
- Wortmann U. G., Bernasconi S. M. and Böttcher M. E. (2001) Hypersulfidic deep biosphere indicates extreme sulfur isotope fractionation during single-step microbial sulfate reduction. *Geology* **29**, 647–650.

Associate editor: Martin B. Goldhaber